Performance Evaluation of SWIPT-enabled Cellular Networks with Adaptive Modulation -A Stochastic Geometry Approach

Lam-Thanh Tu, Abbas Bradai, Yannis Pousset

JS 20 FUTURE NETWORKS: 5G AND BEYOND

Performance Evaluation of SWIPT-enabled Cellular Networks with Adaptive Modulation - A Stochastic Geometry Approach

L'évaluation des performances des réseaux cellulaires compatibles SWIPT avec modulation adaptative - Une approche de la géométrie stochastique

***Lam-Thanh Tu*[1], *Abbas Bradai*[2], *and Yannis Pousset*[3]**

[1] *XLIM, University of Poitiers, lam.thanh.tu@univ-poitiers.fr*
[2] *XLIM, University of Poitiers, abbas.bradai@univ-poitiers.fr*
[3] *XLIM, University of Poitiers, yannis.pousset@univ-poitiers.fr*

Keywords: SWIPT, Adaptive Modulation, Performance Analysis, Stochastic Geometry
Mots clés : SWIPT, Modulation adaptive, Aanalyse de performance, Géométrie stochastique

Abstract:
The performance of simultaneous wireless information and power transfer (SWIPT)-enabled cellular networks by utilizing adaptive modulation are investigated. In particular, the coverage probability (Pcov), the occurrence probabilities of different mode of modulations and the achievable spectral efficiency (ASE) are provided by leveraging tools from stochastic geometry. It should be noted that different from works in the literature which are ignored the spatial-correlation between base stations (BSs) as well as the correlation between information decoding and harvested energy at the end-devices (EDs), we take these into considerations by yielding the recent definition of the coverage probability. Finally, our numerical results show that employing adaptive modulation in SWIPT-enabled ED is a promising way to improve both spectral efficiency (SE) and energy efficiency (EE) of cellular networks.
Résumé :
Les performances des réseaux cellulaires activée par SWIPT (Simultaneous wireless Information and Power Transfer) en utilisant la modulation adaptative sont étudiées. En particulier, la probabilité de couverture (Pcov), les probabilités d'occurrence des modes configurations de modulation différentes et l'efficacité spectrale souhaitée (ASE) sont fournies en exploitant des approches de la géométrie stochastique. Il convient de noter qu'à la différence des travaux de la littérature qui ignorent la corrélation spatiale entre les stations de base (BS) ainsi que la corrélation entre le décodage des informations et l'énergie récoltée au niveau des dispositifs finaux (ED), nous les prenons en considération en donnant la définition récente de la probabilité de couverture. Enfin, nos résultats numériques montrent que l'utilisation de la modulation adaptative dans les ED compatibles SWIPT est un moyen prometteur d'améliorer à la fois l'efficacité spectrale (SE) et l'efficacité énergétique (EE) des réseaux cellulaires.

1 Introduction

Nowadays, one of main challenges of end-devices (EDs) is how to prolong its operation over a reasonable amount of time. At the first attempt, a larger battery seems to be an appropriate solution, it, however, typically leads to the devices itself too bulky. In addition, some special EDs may even not be able to re-charge its battery, such as sensor nodes that operate under harsh environment. In this context, energy harvesting (EH) is regarded as a promising technology to address this problem. Among all available EH techniques, the simultaneous wireless information and power transfer (SWIPT) is emerging as a suitable solution for end-devices thanks to its cost-effective and utilizing the available energy sources like interference from other concurrent transmission, compared with other EH solutions, i.e., power beacon, solar and/or wind energy sources. In particular, in SWIPT, the radio frequency (RF) signals are utilized to not only convey information but also to replenish the battery of the EDs by installing a complement low-cost energy harvester along with the traditional receiver [1].

On the other hand, adaptive modulation is a mature technology which has been proven as a key technique to improve spectral efficiency (SE). Particularly, based on the practical channel conditions, the transmitter actively adjusts its modulation schemes, i.e., BPSK, QPSK, 8PSK and so on, to maximize the data rate thus improving the spectral efficiency, for example, the lower the signal-to-interference-plus-noise ratio (SINRs) is, the smaller the modulation scheme is yielded. As a result, in this work, we investigate the performance of cellular networks at system-level by applying both SWIPT and adaptive modulation. It should be noted that different from the traditional approach which uses system simulator to obtain the results at system-level. Our work, on the other hand, studies the performance of system-level cellular networks by leveraging the advantages of tools from stochastic geometry (SG) which is proven to be more tractable and consuming less resources compared with the system simulator approach [2].

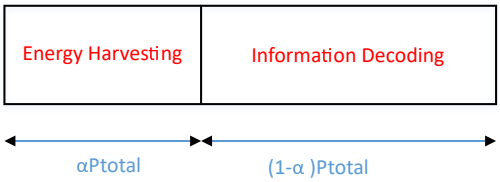

Figure 1 – Illustration of the power-splitting (PS) protocol of SWIPT-enabled receiver.

1.1 Related works

In this section, the state-of-the-art of both SWIPT and adaptive modulation at system-level cellular networks are discussed. In [3] the energy efficiency (EE) of SWIPT-enabled multi-cell multiple-input single-output (MISO) networks was investigated. In particular, a centralized beamforming scheme is designed by using the semi-definite relaxation and successive convex approximation technique to maximize the EH efficiency. The ergodic capacity of SWIPT hybrid non-orthogonal multiple access (NOMA) system was addressed in [4]. This work, however, merely studied the performance at link-level instead of system-level. Furthermore, the interference-free system is considered which is not true in practical cellular networks. The outage probability of SWIPT NOMA system with transmit antenna selection was taken into consideration in [5]. Nevertheless, this work also ignores the presence of interference as well as no adaptive modulation is considered.

The performance of both mmWave and computational radio frequency identification networks were provided in [6, 7]. Although stochastic geometry is utilized to modelling the EDs in [6], the metrics of interest, nonetheless, are the power condition and information condition instead of either coverage probability (Pcov) or achievable spectral efficiency (ASE) as in our work. Compared with [7], we do not consider the help of relay but adaptive modulation is taken into account.

One of the seminal works that investigates the performance of adaptive modulation in cellular networks was [8], in this work, however, energy harvesting is not considered and the networks was modelled by rectangular grid modelling which is too ideal to model the cellular networks. Other works, i.e., [9, 10], investigated different aspects of cellular network with adaptive modulation. To be more specific, the EE of two-tier multiple-input multiple-output (MIMO) cellular networks was investigated in [9] while [10] studied the performance of adaptive multicast mechanism. Our work, on the contrary, is considered different scenarios. The main contributions as well as novelties are provided in the sequel.

1.2 Main contributions and novelties

In this paper, different to the above-mentioned works, we study the performance of SWIPT-enabled cellular networks at system-level by applying adaptive modulation. Particularly, the main contributions and novelties of this manuscript are summarized as follows:

- Tools from stochastic geometry are used to modelling the distributions of both EDs and base stations (BSs).
- Nakagami-m fading is taken into account instead of Rayleigh fading to better modelling the channel coefficient.
- Power-splitting (PS) SWIPT protocol is taken into consideration.
- Adaptive modulation is utilized to actively exploit the channel state information (CSI) at the BS.
- Three performance metrics are investigated, namely, the coverage probability, the occurrence probabilities of different modulation schemes, and the achievable spectral efficiency are studied and compared with the baseline system, fixed modulation.
- A recent definition of coverage probability is yielded which is able to take into consideration both harvested energy and information decoding.
- Different to the works in the literature, spatial-correlation are considered via the harvested power and information decoding.

2 Systems models

2.1 Cellular Network Modelling

Let us consider a downlink cellular networks where the BSs are modelled according to a homogeneous Poisson point process (PPP) denoted by Ψ_{BS} with density λ_{BS}. The EDs, in addition, is also modelled by

another homogeneous PPP which is independent of Ψ_{BS} and denoted by Ψ_{ED} with density λ_{ED}. It should be emphasized that in this paper, the general scenario is considered rather than fully-loaded as most of the work in the literature [11].

The performance is measured at the typical ED denoted by, ED_0, which is located at the origin of the two-dimensional plane. According to Palm theory [12], the results measure at ED_0 can be applied to other EDs of the networks. The total receive power at the ED_0, which includes both intended and interference BS, is divided into two different parts thanks to power-splitting (PS) protocol as illustrated in Fig. 1. Let us denote P_{total} at the total receive power at ED_0. A fraction of the receive power, $\alpha P_{\mathrm{total}}$, $\alpha \in (0,1)$, is put into the energy harvester to charge the battery, where α is the power splitting ratio. The remain part, i.e., $(1-\alpha)\,P_{\mathrm{total}}$, is used to decode the incoming information from the serving BS denoted by BS_0. It is noted that depending on the channel gain which can be obtained via the simultaneous and error-free channel state information[1], BS_0 selects an appropriate modulation scheme to transmit to the ED_0. Moreover, the results can also be extended straightforwardly to time switching (TS) and antenna switching (AS) protocols, respectively [13, Section. 1.5.1]. In this work, we assume that orthogonal resources allocations are considered inside each-cell. It means that there is no intra-interference in each cell, nevertheless, other-cell interference, of course, is considered.

2.2 Small-scale fading and large-scale path-loss modelling

Let us consider the generic link from BS-to-ED. The wireless signal is degraded by both small-scale fading and large-scale path-loss. The impact of shadowing is studied implicitly by modifying the density of the BS [14].

2.2.1 Small-scale fading

The small-scale fading of the generic link from BS-to-ED is assumed to follow Nakagami-m fading with shape and spread parameters denoted by m and Ω, respectively. The channel gain, as a result, denoted by h_n, is followed Gamma distribution with shape and scale meters denoted by k and $\theta = \frac{\Omega}{m}$.

2.2.2 Large-scale path-loss

Let us consider the generic link between an arbitrary BS and ED. The large-scale path-loss, denoted by L_n, is computed by applying unbounded path-loss model and is formulated as follows:

$$L_n = l\left(r_n\right) = \mathcal{K}_0 r_n^{\beta} \tag{1}$$

where $\mathcal{K}_0$ is the path-loss constant and is computed as $\mathcal{K}_0 = \left(\frac{4\pi f_c}{3\times 10^8}\right)^2$, where f_c is the carrier frequency and the number 3×10^8 (in meter per second) is the speed of light; $\beta > 2$ is the path-loss exponent.

It is apparent that general path-loss models, such as, the bounded path-loss model and/or the multiple path-loss exponent and so on, can be taken into consideration. Nonetheless, in this work, for simplicity, the basic and widely applied path-loss model is yielded.

2.2.3 Cell association

As far as the cell association is concerned, the smallest path-loss denoted by $L^{(0)}$, is utilized as a criteria to select the serving BS, BS_0, and is formulated as

$$L^{(0)} = \min_{n\in\Psi_{\mathrm{BS}}} \left\{l\left(r_n\right)\right\} \tag{2}$$

The core reason for applying this criteria instead of other advanced standards, i.e., the highest received power, is that it consumes less power at the ED since the ED does not always keep measuring the channel coefficient from all BSs. In fact, it requires only the distance from the ED to the BS.

2.3 Adaptive Discrete Modulation

Adaptive discrete modulation is one of key solutions to improve spectral efficiency by actively exploiting the advantages of channel state information at the transmitter (CSIT). Under the considered networks, we assume that this information is error-free and no delay as well. In particular, depending on the signal-to-interference-plus-noise ratio (SINR) at the receiver, the BS chooses the most appropriate modulation scheme to transmit

[1]In general, this assumption is idealistic, thus, the results in this paper can be deemed to represent the upper-bound of the practical scenarios.

information. Let us split the entire range of SINR into $\mathcal{A} \in \mathbb{N}$ non-overlapping region and the boundary of each interval is denoted by γ_{T}^{a}, $a \in \{0, \ldots, \mathcal{A}\}$, as follows:

$$0 = \gamma_{\mathrm{T}}^{0} < \gamma_{\mathrm{T}}^{1} < \ldots < \gamma_{\mathrm{T}}^{a} < \ldots < \gamma_{\mathrm{T}}^{\mathcal{A}} = +\infty \tag{3}$$

In this work, the popular M-QAM modulation scheme is taken into account. In particular, $M_k = 2^k$-QAM modulation is selected if the SINR drops into the interval $\left[\gamma_{\mathrm{T}}^{k}, \gamma_{\mathrm{T}}^{k+1}\right)$, $k \in \{1, \ldots, \mathcal{A}-1\}$. In addition, if the SINR is extremely small or it belongs to the region $\left[\gamma_{\mathrm{T}}^{0} = 0, \gamma_{\mathrm{T}}^{1}\right)$, BS stops transmitting and the outage event appears.
In order to identify the boundary values, the bit error rate of M-QAM with Gray coding over AWGN channel is applied as follows [15]:

$$\mathrm{BER}_T = \varsigma_k \, Q\left(\sqrt{\tau_k \gamma_{\mathrm{T}}^{k}}\right) \Rightarrow \gamma_{\mathrm{T}}^{k} = \frac{1}{\tau_k}\left[Q^{-1}\left(\frac{\mathrm{BER}_T}{\varsigma_k}\right)\right]^2, \quad k \in \{1, \ldots, \mathcal{A}-1\}, \tag{4}$$

where $Q(.)$ and $Q^{-1}(.)$ are the Gaussian Q function and the inverse Gaussian Q function, respectively; BER_T is the intended bit error rate threshold; and

$$\varsigma_k = \begin{cases} 1 & m_k = 1, 2 \\ 4/m_k & m_k \geq 3 \end{cases}, \quad \tau_k = \begin{cases} 2/m_k & m_k = 1, 2 \\ 3/\left(2^{m_k} - 1\right) & m_k \geq 3 \end{cases} \tag{5}$$

where $m_k = \log_2(M_k)$.

2.4 Energy Harvesting

The harvested energy denoted by $\mathcal{EH}$ (in Joule), is the total received power from all active BSs at the ED and is formulated as follows [16]:

$$\mathcal{EH} = \alpha\eta \left(P_{\mathrm{BS}} \sum_{i \in \Psi_{\mathrm{BS}}^{(\mathrm{A})}} \frac{h^{(i)}}{L^{(i)}} \right). \tag{6}$$

Here $\eta \in [0, 1]$ is the energy conversion coefficient; P_{BS} is the transmit power of the BSs; $\Psi_{\mathrm{BS}}^{(\mathrm{A})}$ is the set of active BS which is also considered as an homogeneous PPP with density $\lambda_{\mathrm{BS}}^{\mathrm{A}} = \left(1 - \left(1 + \frac{1}{3.5}\frac{\lambda_{\mathrm{ED}}}{\lambda_{\mathrm{BS}}}\right)^{-3.5}\right)\lambda_{\mathrm{BS}}$ [17]. Under the considered networks, the BS is considered as active if at least one MT is located at its Voronoi cell. $h^{(i)}$ and $L^{(i)}$ are the small-scale fading and the large-scale path-loss from the i-BS to the typical ED, respectively. In Eq. (6), the AWGN noise at the receiver is ignored since the power harvests from noise is not comparable with the interference.

2.5 Signal-to-Interference-Plus-Noise Ratio

The SINR at ED_0 is formulated as follows

$$\gamma_{\Delta} = \frac{P_{\mathrm{BS}} \frac{h^{(0)}}{L^{(0)}}}{P_{\mathrm{BS}} \sum\limits_{j \in \Psi_{\mathrm{BS}}^{(\mathrm{A})} \setminus (0)} \frac{h^{(j)}}{L^{(j)}} + \sigma_{\mathrm{N}}^2 + \sigma_{\mathrm{C}}^2} \tag{7}$$

where $\sigma_{\mathrm{N}}^2 = -174 + \mathrm{NF} + 10\log_{10}(\mathrm{BW})$ (in dBm) is the AWGN noise variance at the ED_0; BW is the transmission bandwidth; NF is the noise figure at the ED; $\sigma_{\mathrm{C}}^2 = \frac{\sigma_{\mathrm{cov}}^2}{(1-\alpha)}$ [18], where σ_{cov}^2 refers to the noise introduced during the conversion from radio frequency (RF) signal to baseband; and $h^{(s)}$, $L^{(s)}$, $s \in \{0, j\}$, are the small-scale fading and the large-scale path-loss from the BS_s to ED_0; $\Psi_{\mathrm{BS}}^{(\mathrm{A})} \setminus (0)$ is a set of active BS except for BS_0.

3 Performance Metrics

3.1 Coverage Probability

In this section, three performance metrics are investigated, i.e., the coverage probability, the occurrence probabilities of different modulation schemes, and the achievable spectral efficiency of each ED. In particular, the coverage probability, Pcov, is defined as the number of successful transmission over the total transmission.

TABLE I: Setup of parameters (unless otherwise stated)

Parameters [Unit]	Values
Rcell $= \frac{1}{\sqrt{\pi\lambda_{\mathrm{BS}}}}$ [m]	40
RED $= \frac{1}{\sqrt{\pi\lambda_{\mathrm{ED}}}}$ [m]	100
P_{BS} [dBm]	30
BER_T	10^{-3}
γ_{E} [dBm]	-80
BW [kHz]	250
η	0.7
α	0.3
$\mathcal{A}$	5
NF [dB]	10
σ^2_{cov} [dBm]	-70
m	4.5
Ω	12.5
β	3.5
f_c [GHz]	2.1

However, different from most of works in the literature, the Pcov under the considered cellular networks occurs providing that two following conditions are satisfied simultaneously: i) The probability that the harvested energy is greater than an activation threshold; ii) The probability that the receive SINR is greater than γ_T^1 and is formulated as follows:

$$\mathrm{Pcov} = \Pr\left\{\mathcal{EH} \geq \gamma_{\mathrm{E}}, \gamma_{\Delta} \geq \gamma_{\mathrm{T}}^1\right\} \tag{8}$$

Here γ_{E} is the predefined energy threshold so that the ED is activated. It is apparent that Eq. (8) is recently proposed. The benefits of this recent definition is that it takes into account both energy harvesting and SINR together in lieu of separately.

3.2 Occurrence probabilities of each modulation scheme

The probability that the BS_0 transmits at k modulation scheme refers to the occurrence probabilities denoted by Υ_k and is computed as

$$\Upsilon_k = \Pr\left\{\mathcal{EH} \geq \gamma_{\mathrm{E}}, \gamma_{\mathrm{T}}^k \leq \gamma_{\Delta} \leq \gamma_{\mathrm{T}}^{k+1}\right\}, \quad k \in \{1, \ldots, \mathcal{A}-1\}. \tag{9}$$

It should be noted the sum of Υ_k where $k \in \{0, \ldots, \mathcal{A}-1\}$ is equal to one. Mathematical speaking, we have

$$\sum_{k=0}^{\mathcal{A}-1} \Upsilon_k = 1. \tag{10}$$

3.3 Achievable Spectral Efficiency (ASE)

Under adaptive modulation system, the average link achievable spectral efficiency (ASE) (in bits/s/Hz) can be computed as a weighted sum of the data rate associated with $\mathcal{A}$ region as follows [19]:

$$\mathrm{ASE} = \sum_{k=1}^{\mathcal{A}-1} m_k \Upsilon_k. \tag{11}$$

4 Numerical Results

In this section, numerical results are provided to measure the performance of these above metrics, i.e., Pcov and ASE. Without loss of generality, the simulation parameters are provided in Table I. In Table I, Rcell and RED are the inter-site distance between BSs and average distance between two EDs, respectively. In this work, five adaptive modulation scheme are applied as [19], namely, no transmission, BPSK, QPSK, 16QAM and 64QAM, respectively. It should be noted that different kinds of modulations as well as higher modulation levels can be employed straightforwardly.

Fig. 2 reveals the behaviour of Pcov respect to both energy harvesting threshold, γ_{E}, and BER threshold, i.e., BER_T. We experience that the Pcov is a concave function of both variables. In addition, the Pcov is

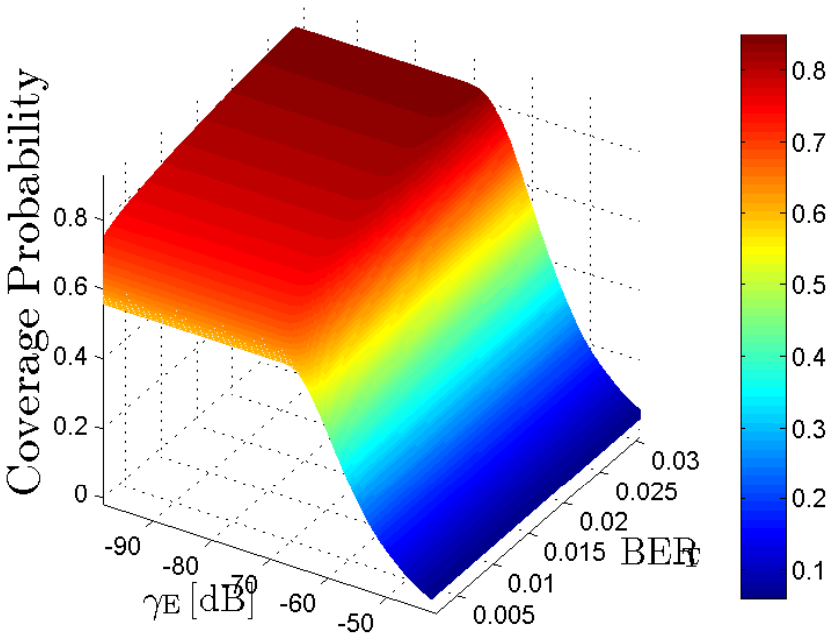

Figure 2 – Pcov as a function of both energy harvesting threshold, γ_{E}, and BER threshold, BER_T.

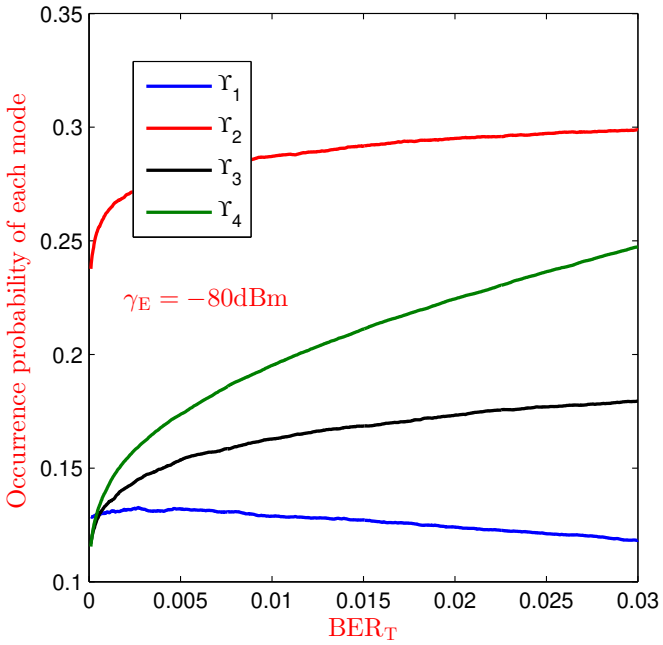

Figure 3 – Occurrence probabilities vs BER threshold, BER_T. $\Upsilon_k = \{\mathrm{BPSK}, \mathrm{QPSK}, 16\mathrm{QAM}, 64\mathrm{QAM}\}$, $k \in \{1, 2, 3, 4\}$.

monotonically decreasing with γ_{E} providing that BER_T is constant. The same pattern can be obtained if γ_{E} is fixed and BER_T reduces.

The occurrence probabilities, Υ_k, is shown in Fig. 3 versus the bit error rate threshold, BER_T. The results show that Υ_2 or QPSK always outperforms others modulation schemes. Furthermore, it is obvious that the lower the BER_T threshold is, the higher the probability of 64QAM or Υ_4 is attained.

Fig. 4 illustrates the performance of ASE as a function of energy requirement. It is no doubt that ASE is monotonically decreasing with γ_{E}. Furthermore, it is easy to recognize that the proposed adaptive modulation outperforms all fixed modulations from BPSK to 64QAM. To be specific, the performance of the proposed scheme is almost two-fold compared with 16QAM modulation and around three-times if BPSK is used. Finally, it is apparent that increasing BER threshold will reduce the ASE as expected.

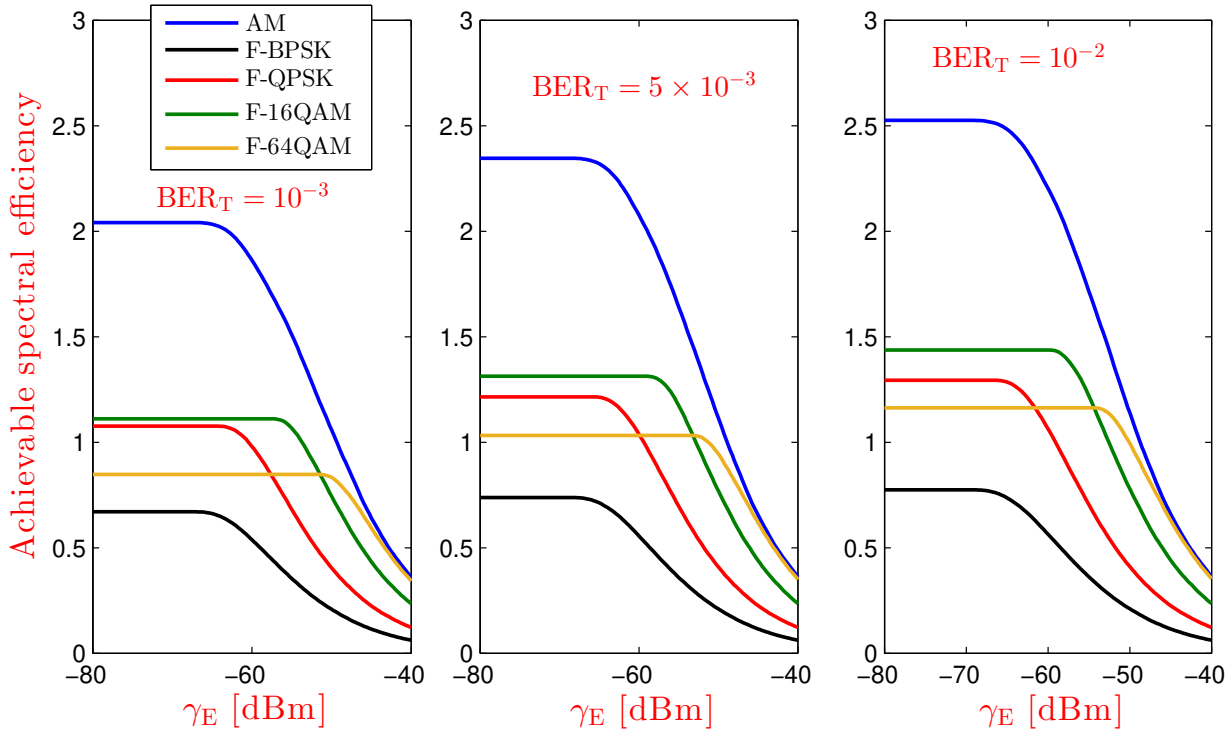

Figure 4 – Achievable spectral efficiency of the proposed adaptive modulation and fixed modulation versus energy harvesting threshold γ_E with various value of BER$_T$. Here, AM denotes the proposed adaptive modulation; F-k, $k \in \{\text{BPSK}, \text{QPSK}, \text{16QAM}, \text{64QAM}\}$ denotes fixed k modulation, i.e., F-BPSK is fixed BPSK modulation.

5 Conclusion

In this paper, the performance of cellular networks is investigated with three metrics, coverage probability, occurrence probabilities and achievable spectral efficiency, correspondingly. In particular, five discrete modulation schemes are considered, no transmission, BPSK, QPSK, 16QAM and 64QAM respectively. The results show that by applying adaptive modulation as well as the energy harvesting, we are able to increase both spectral efficiency and energy efficiency. These performances can be enhanced significantly by considering network slicing with the current infrastructure [20] or using deep learning combined with mathematical modelling [21].

6 References

[1] J. Huang, C.-C. Xing, and C. Wang, "Simultaneous wireless information and power transfer: Technologies, applications, and research challenges," *IEEE Commun. Magazine*, vol. 55, pp. 26–32, Nov. 2017.

[2] M. Haenggi, *Stochastic Geometry for Wireless Networks*. Cambridge University Press, 2012.

[3] S. Jang, H. Lee, S. Kang, T. Oh, and I. Lee, "Energy efficient swipt systems in multi-cell miso networks," *IEEE Trans Commun.*, vol. 17, pp. 8180–8194, Dec. 2018.

[4] S. K. Zaidi, S. F. Hasan, and X. Gui, "Evaluating the ergodic rate in swipt-aided hybrid noma," *IEEE Commun. Lett.*, vol. 22, pp. 1870–1873, Sep. 2018.

[5] T. N. Do, D. B. Costa, T. Q. Duong, and B. An, "Improving the performance of cell-edge users in miso-noma systems using tas and swipt-based cooperative transmissions," *IEEE Trans. Green Commun. Netw.*, vol. 2, pp. 2473–2400, Mar. 2018.

[6] Y. Kim, T. J. Lee, and D. I. Kim, "Joint information and power transfer in swipt-enabled crfid networks," *IEEE Wireless Commun. Lett.*, vol. 7, pp. 186–189, Apr. 2018.

[7] S. Biswas, S. Vuppala, and T. Ratnarajah, "On the performance of mmwave networks aided by wirelessly powered relays," *IEEE J. Sel. Areas Commun.*, vol. 10, pp. 1522–1537, Dec. 2016.

[8] X. Qiu and K. Chawla, "On the performance of adaptive modulation in cellular systems," *IEEE Trans. Commun.*, vol. 47, pp. 884–895, Jun. 1999.

[9] R. H. Aquino, S. A. R. Zaidi, D. McLernon, and M. Ghogho, "Energy efficiency analysis of two-tier mimo diversity schemes in poisson cellular networks," *IEEE Trans. Commun.*, vol. 63, pp. 3898–3911, Oct. 2015.

[10] M. Li and Y. H. Wu, "Performance analysis of adaptive multicast streaming services in wireless cellular networks," *IEEE Trans. Mobile Comput.*, vol. 18, pp. 2616–2630, Nov. 2019.

[11] J. G. Andrews, F. Baccelli, and R. K. Ganti, "A tractable approach to coverage and rate in cellular networks," *IEEE Trans. Commun.*, vol. 59, pp. 3122–3134, Nov. 2011.

[12] M. Haenggi, *Stochastic Geometry for Wireless Networks*. Cambridge University Press, 2013.

[13] L. T. Tu, *New Analytical Methods for the Analysis and Optimization of Energy-Efficient Cellular Networks by Using Stochastic Geometry*. PhD thesis, University of Paris-Sud, 6 2018.

[14] M. D. Renzo, A. Zappone, L.-T. Tu, and M. Debbah, "System-level modeling and optimization of the energy efficiency in cellular networks – a stochastic geometry framework," *IEEE Wireless Commun.*, vol. 17, pp. 2539–2556, Apr. 2018.

[15] V. N. Q. Bao and H. Y. Kong, "Joint adaptive modulation and distributed switch-and-stay for partial relay selection networks," *IEICE Trans. Commun.*, vol. 95, pp. 668–671, Feb. 2012.

[16] L.-T. Tu, M. D. Renzo, and J. P. Coon, "System-level analysis of swipt mimo cellular networks," *IEEE Commun. Lett.*, vol. 20, pp. 2011–2014, Oct. 2016.

[17] S. M. Yu and S.-L. Kim, "Downlink capacity and base station density in cellular networks," in *IEEE Workshop on Spatial Stochastic Models for Wireless Networks*, pp. 1–7, 5 2013. [Online]. Available: http://arxiv.org/pdf/1109.2992.pdf.

[18] L.-T. Tu, M. D. Renzo, and J. P. Coon, "System-level analysis of receiver diversity in swipt-enabled cellular networks," *IEEE/KICS J. Commun. Netw.*, vol. 18, pp. 926–937, Dec. 2016.

[19] M. S. Alouini and A. Goldsmith, "Adaptive modulation over nakagami fading channels," *Wireless Pers. Commun.*, vol. 13, pp. 119–143, May. 2000.

[20] S. Dawaliby, A. Bradai, and Y. Pousset, "Distributed network slicing in large scale iot based on coalitional multi-game theory," *IEEE Trans. Netw. Service Manag.*, vol. 16, pp. 1567 – 1580, Dec. 2019.

[21] A. Zappone, M. D. Renzo, M. Debbah, L. T. Tu, and X. Qian, "Model-aided wireless artificial intelligence: Embedding expert knowledge in deep neural networks for wireless system optimization," *IEEE Veh. Technol. Mag.*, vol. 14, pp. 60–69, Sep. 2019.